Hadronic Final States & QCD Working Group summary

G. Hesketh[1], A. Knutsson[2] and L. Motyka[3,4]

1- Northeastern University – Physics Department
111 Dana Research Center, Boston, MA, 02115, USA

2- DESY
Notkerstrasse 85, D-22603 Hamburg, Germany

3- II Institute for Theoretical Physics, University of Hamburg,
Luruper Chaussee 149, D-22761, Germany

4- Institute of Physics, Jagellonian University,
Reymonta 4, 30-059 Kraków, Poland

The QCD and Hadronic Final State working group session [1] at the DIS 2009 workshop is summarised.

1 Introduction

At the advent of the LHC, experimental particle physics will enter a new kinematic regime. The high energy proton collisions there will allow further tests of the Standard Model, and searches for new physics which was inaccessible to previous experiments. A precise description of the hadronic final state is one of the key elements in carrying out these studies. For example, the Higgs boson signal is expected to appear on the top of a strong background coming from final states involving jets, electroweak bosons and leptons. Therefore it is vital to achieve a good theoretical understanding of these final states, and a detailed, efficient and accurate full simulation of such events. This understanding has developed through advances in both theoretical and experimental fields, and many new results were presented in the QCD and Hadronic Final State working group.

A broad range of hadronic processed have been calculated within a QCD formalism based on collinear factorization. The relevant hard matrix elements are typically known at next-to-leading order (NLO) accuracy in perturbative QCD, with some even evaluated at next-to-next-to-leading (NNLO) order. Parton densities are strongly constrained by experimental measurements, and their evolution is now known at NNLO accuracy. For some observables, for which higher order corrections are strongly enhanced by logarithmic factors, resummation techniques may be applied. In result, the relevant differential cross sections are typically known with good or very good accuracy.

To go from these calculations to simulated events, several Monte Carlo computer codes are available. These codes often also dress the hard scattering with non-perturbative effects, such as hadronization and a model of the proton remnants and multiple parton interactions (the underlying event). The codes are tested against the existing data and provide good description of many important observables. The increasing precision of these experimental tests are seen in new measurements from HERA, which make use of the high statistics from the so called HERA II run together with an improved understanding of the detectors. The HERA measurements achieve experimental errors which in some cases are much lower than the theoretical errors. Also at the Tevatron, where the unprecedented accuracy in jet energy scale determination is leading to very precise jet measurements, constraining the

distribution of gluons carrying a large fraction of proton momentum and any signs of new physics entering at the highest energies.

However, such integration of the hard cross section and non-perturbative models in Monte Carlo is sometimes only available for leading order calculations, particularly for the important vector boson plus jet final state which suffer much more significant theoretical uncertainites. Further, there are some uncertainties in the extrapolation of the underlying event models to LHC energies. New results also test these important areas.

2 Experiment: *ep*

A wide range of different final state measurements in *ep* physics were covered by in total 17 presentations. The main topics were measurements with hadronic final state jets, prompt photons, charged particles and strange particles from the H1 and ZEUS collaborations. Talks on measurements with fixed targets were presented by the CLAS and HERMES collaborations. The measurements show that we understand the final state in *ep* collisions well, but we sometimes lack precision and higher orders in the fixed order calculations.

2.1 Jet physics

Both H1 and ZEUS collaboration presented new measurements of jet cross sections. The measurements are used to extract $\alpha_s(M_Z)$ with a higher experimental precision than ever at HERA. ZEUS presented a new jet measurements, based on HERA II data, of inclusive jet production in neutral current (NC) DIS for photon virtualities $Q^2 > 125$ GeV^2 and jets with transverse momenta $E_{T,\mathrm{Breit}} > 8$ GeV. [2] In Fig. 1 the cross section is shown as a function of Q^2. The NLO $O(\alpha_s^2)$ calculation describes the data well. The value of $\alpha_s(M_Z)$ extracted from the measurement in the region $Q^2 > 500$ GeV^2 is $\alpha_s(M_Z) = 0.1192 \pm 0.0014(stat)\,^{+0.0035}_{-0.0033}(exp)\,^{+0.0022}_{-0.0023}(th)$.

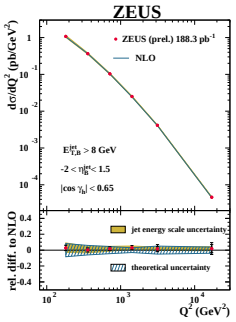

Figure 1: Inclusive jet cross sections in NC DIS compared to a NLO $O(\alpha_s^2)$ calculation. [2]

H1 has measured normalized cross sections for inclusive jet, 2-jet and 3-jet production in NC DIS in the range $150 < Q^2 < 15000$ GeV^2 using both HERA I and II data. [3] The different normalized cross sections are well described by the NLO calculations, and the uncertainty of the calculations are clearly larger than the experimental uncertainties in many bins. A combined fit to the inclusive, 2- and 3-jet normalized cross section gives $\alpha_s(M_Z) = 0.1168 \pm 0.0007(exp)\,^{+0.0046}_{-0.0030}(th) \pm 0.0016(PDF)$. The experimental error, which is dominated by the

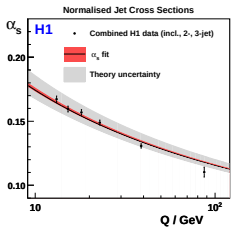

Figure 2: Values of $\alpha_s(Q)$ obtained from a combined fit of inclusive jet, 2- and 3-jet normalised cross sections. [3]

hadronic energy scale uncertainty, is below 1%. Fig. 2 shows the running of $\alpha_s(Q)$ for the combined fit and the Q^2 bins used in the measurement.

ZEUS has analysed the substructure in jets in NC DIS events with $Q^2 > 125$ GeV^2. [4] Sub-jets are defined by reapplying the inclusive k_t-algorithm to particles inside the jets. Normalised sub-jet cross sections were measured and compared to NLO or LO ($O(\alpha_s^2)$) predictions for jets with two or three sub-jets, respectively. In Fig. 3 the sub-jet cross sections for jets with two sub-jets are shown as a function of the difference in pseudorapidity between the jet and respectively sub-jet. The data are well described by the calculations, and as seen the hardest sub-jets goes in the forward region. The results supports the expectations from color coherence effects. The cross sections for jets with 3-subjets are described somewhat worse by the LO calculations, but still adequately.

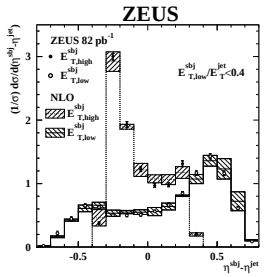

Figure 3: Nomalised sub-jet cross sections as a function of the rapidity difference between the jet and the sub-jets. The data are compared to NLO $O(\alpha_s^2)$ calculations. [4]

In another measurement by ZEUS [5] angular correlations in three-jet events are used to test QCD and study color configurations in both photoproduction and DIS. Several symmetry groups were tested and compared to the data for different angular variables. Color configurations predicted by SU(3) describe the analysed data best, while other symmetry groups are disfavoured.

2.2 Prompt Photons

Final states with an isolated photon have been analysed by H1, in photoproduction ($Q^2 < 1$ GeV^2) [6], and ZEUS in NC DIS ($10 < Q^2 < 350$ GeV^2) [7]. The identification of the photons are based on shower shape variables and the isolation criteria is that the photon carries at least 90% of the energy of the jet containing the photon. The measurements are compared to various theoretical calculations. The DIS cross sections are in addition compared to MC models with parton showers.

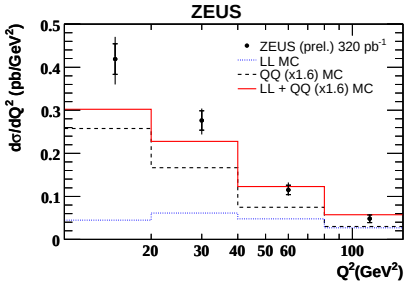

Figure 4: Cross-section for prompt photons in NC DIS as a function of Q^2. The data are compared to predictions from MC with parton showers. The MC predictions are separated into photon radiation from leptons (LL) and quarks (QQ), and the sum of these. [7]

In photoproduction a calculation based on the k_t-factorisation approach [8] describes the data best, while a NLO QCD prediction [9] fails to describe the cross sections for backward photons. When an additional jet is required in the event both calculations fail at low pseudorapidities and in particular the description of the correlation in azimuthal angle and transverse momenta between the photon and the jet is not sufficient.

In the DIS analysis, a LO ($O(\alpha_{\rm em}^3)$) calculation [10], which takes the contribution from initial and final state photon radiation from leptons and quarks into consideration, and also includes quark to photon fragmentation, underestimates the prompt photon cross sections. A calculation from the MRST group [11], with the photon radiation from leptons enhanced, fails to describe the shape of the data cross sections. The best description of the DIS data is provided by Monte Carlo models with parton showers after that the contribution from photon radiation from quarks has been scaled. However, as for the fixed order calculations, the MC predictions fail at low Q^2 and x. This is illustrated in Fig. 4.

2.3 Measurements with Charged Particles

The charge asymmetry of particles in the hadronic final state was investigated by the H1 collaboration in NC DIS in the kinematic range $100 < Q^2 < 8000$ GeV^2. [12] Fig. 5a) shows the normalized distribution, $D(x_p)$, of the scaled particle momentum, $x_p = \frac{2p}{Q}$, for positive (pos) and negative (neg) charged particles as well as the sum of the two. Fig. 5b) shows the charge particle asymmetry, $(pos - neg)/(pos + neg)$, compared to various models. At large x_p, where the produced particles retain the information from the hard interactions with sea quarks and gluons, a large charge asymmetry is seen. At low x_p the particles produced in the fragmentation process play an important role, and the asymmetry is smaller. This is also seen in Fig. 5c) where the MC prediction with hadronization turned off (CDM-quark) maintain the charge asymmetry at low x_p.

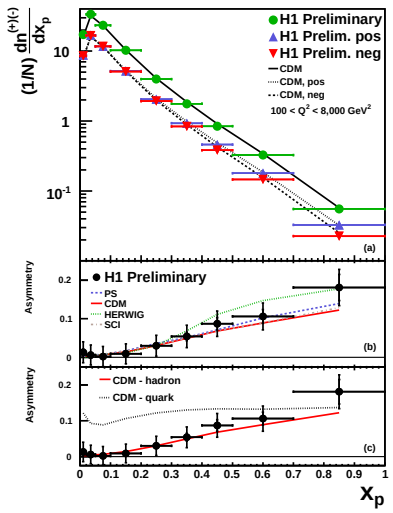

Figure 5: Scaled momentum distributions for positive and negative particles, and the asymmetry between these, compared to various MC models with parton showers.

ZEUS collaboration measures the scaled momentum distributions of charged particles in dijet events in photoproduction ($Q^2 < 1$ GeV^2). [13] The measurement is done for particles inside cones around the dijets, where the fragmentation is expected to be valid. By making fits to the peaks of the scaled momentum distributions the universal scale in the Modified Leading Log Approximation, $\Lambda_{\rm eff}$, and the Local Parton Hadron Duality parameter, κ^{ch}, have been extracted.

H1 investigates the underlying event (UE) in tagged photoproduction ($Q^2 < 0.01$) [14] and uses an approach similar to the UE analyses performed at the Tevatron. The average multiplicity of charged particles in jet events is measured in different azimuthal regions with respect to the leading jet. In regions transverse to the leading jet, the contribution from multiparton interactions (MPI) is largest. In these regions MPI simulations need to be included in PYTHIA [15] in order to describe the data. Remarkable is that the data description provided by CASCADE [16], a MC generator with parton showers based on the k_t-factorisation approach, but without any MPI simulated, is in competition with the predictions from

PYTHIA with MPI.

2.4 Strangeness and Meson Production

Measurements on strangeness production give direct information about fragmentation parameters and knowledge of hadronization. $K^{*\pm}$, K^0_s and Λ productions are analysed by H1 in low Q^2 NC DIS events. [17, 18] One of the cross sections for $K^{*\pm}$ production is shown in Fig. 6 as function of the transverse momentum of the $K^{*\pm}$ in laboratory frame. The MC prediction from DJANGO with the Color Dipole Model (CDM [19]) describes the data well, and also seen is that the largest contribution to the strange quark production comes from the fragmentation. The cross sections for K^0_s and Λ production are compared to Monte Carlo predictions with different values of the strangeness suppression factor λ_s. Although no single combination of model and λ_s describes the data in all kinematic bins, the overall best description of the data is obtained with the CDM and $\lambda_s = 0.3$. Furthermore, the asymmetry between Λ and $\bar{\Lambda}$ production is flat within the errors of the measurement and thus no baryon number transfer from the proton beam to the hadronic final state is observed.

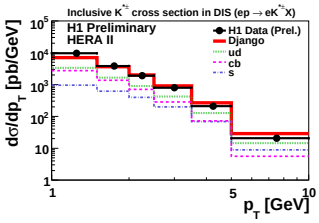

Figure 6: Cross-section for $K^{*\pm}$ production as a function of the transverse momentum of the $K^{*\pm}$s. The MC predictions are decomposed into the contributions of the various quark flavours of the primarily incoming particles of the hard subprocess from the proton side.

H1 presented a measurement of $K^{*\pm}$, ρ^0 and ϕ production in photoproduction ($Q^2 <$ 0.01 GeV). [20] With the average hadronic final state energy ($\langle W_{\gamma p}\rangle \approx 210$ GeV) of the measurement close to the collision energy at RHIC ($\sqrt{s} = 200$ GeV) a comparison to results from RHIC is possible. The ratio of the production cross section between ϕ and K^* agrees very well between the presented measurement and RHIC data. Further, the transverse momentum spectra of the analysed particles are described with the same power law. This supports a thermodynamic picture of the hadronic interaction.

Finally, ZEUS collaboration uses the full HERA data sample (~ 0.5 fb^{-1}) to search for $K^0_s K^0_s$ resonances in over 67000 $K^0_s K^0_s$ pairs in both photoproduction and DIS. [21] Several resonances are observed.

2.5 Fixed target measurements

HERMES and CLAS analyse the hadronic final state in collision between polarised electrons accelerated to 27.5 and up 6 GeV, respectively, and for various fixed targets. Broadening of the transverse momenta of produced hadrons is expected when the particles propagate though matter. This means that a non-zero value is expected for the variable $\Delta\langle p_t^2\rangle^h = \langle p_t^2\rangle^h_A + \langle p_t^2\rangle^h_D$ where $\langle p_t^2\rangle^h$ is the average transverse momentum of the produced particles using Deuterium, D, or a medium with mass number A as target. The effect is observed by both the HERMES [22] and CLAS [23] collaboration for different produced hadrons. The broadening increases with the mass number of the target, but is similar for different produced particles (K^0,π^+, π^-).

CLAS collaboration also presents studies on few nucleon systems. [24] The plateaux in cross sections as a function of the Bjorken scaling variable for different targets normalised to

the Helium cross section give evidence for 2 and 3 nucleon short range correlations. Also preliminary results of searches for color transparency were presented in the talk. Spectroscopy of baryons and mesons at CLAS was presented in [25]. The results include high precision measurements of polarised and unpolarised data in different decay channels. New data of polarisation transferes to the final state were presented.

3 Experiment: $p\bar{p}$ and pp

The high energy frontier is currently being investigated at the Tevatron, a proton anti-proton collider at a center of mass energy of 1.96 TeV. High energy parton-parton interactions are common here, and form the basis of the QCD program. As such processes are calculable to relatively high precision in perturbative QCD, measurements of jet production can be used to constrain parton densities within the proton and search for new interactions. While jet production is the most plentiful process, studies of the colorless photon, W and Z bosons gives further insight into proton structure and partonic interactions. Further, these signals are commonly the irreducible background to searches for the Higgs boson or other new phenomena so accurate simulation of these final states is needed, which follow from data measurements. Experimentally, there are a number of effects that must be understood in order to study these processes. The hadronization of partons into jets much be well modelled, and the experimental jet energy resolution well understood. Further, the role of the proton remnants, additional parton scatters and energy pile-up (referred to as the underlying event) in producing particles or jets in the detector must be understood. New results from the Tevatron in all of these areas were presented.

The LHC will collide protons at a center of mass energy of 14 TeV once design specifications are reached. This increase in energy greatly extends the kinematic reach over the Tevatron, and offers huge potential for exciting new physics. There continues to be an enormous effort in commissioning the LHC experiments in preparation for collisions. Several studies were presented which highlighted status of detector commissioning, and the possibilities to build upon the Tevatron program with a relatively small amount of luminosity from a planned 10 TeV run.

3.1 Underlying Event

Recent results from the Tevatron cover two aspects of the underlying event. D0 presented a new measurement events in which there are two hard parton interactions in a single proton anti-proton collision [26]. The first interaction is tagged with a high energy photon and jet, then events containing two additional hard jets from a second partonic interaction are identified. After accounting for such events caused by multiple collisions in the same bunch crossing, an effective cross section is measured to be 15.1 ± 1.9 pb, which quantifies the reduction in the jet production cross section due to the presence of two hard scatters. CDF presented new studies of charged particle production from the underlying event [27]. The measurement looks at the multiplicity and momenta of particles produced in additions to a Z boson, by dividing the event into azimuthal angular regions transverse and parallel to the Z direction. The regions transverse to the Z tend to contain few particles from the hard scatter, and so are most sensitive to the underlying event. Comparing the same quantities in PYTHIA [15] simulation tuned on dijet production [28] shows good agreement, see Figure 7, suggesting the underlying event is somewhat independent of the hard scattering process.

One of the first measurements to be carried out by ATLAS and CMS will be to repeat these and related studies [29, 30, 31]. Different models and tunes [32, 33] which describe Tevatron data show significant disagreements when extrapolated to LHC energies. Determining the correct model is essential to understanding many basic experimental quantities from lepton isolation to additional energy entering jet cones.

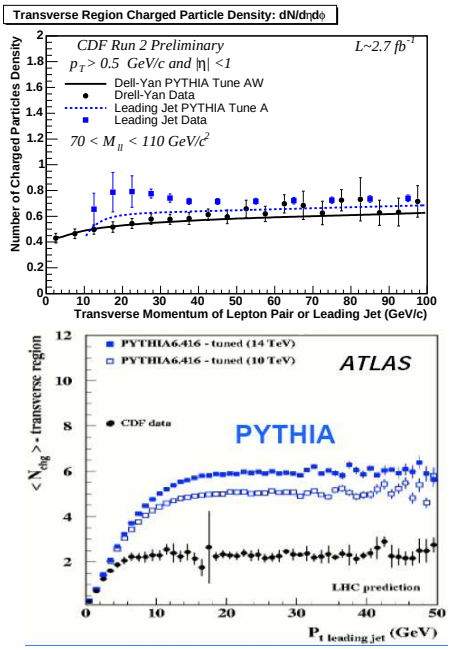

Figure 7: Underlying event measurements at CDF, and studies from ATLAS.

3.2 LHCb Commissioning

The LHCb experiment designed to carry out precise measurements of CP violation, rare decays and heavy flavor physics at the LHC. To obtain the rates of events needed for these measurements, the experiment is designed as a forward spectrometer, covering $1.9 < \eta < 4.9$, and precise vertex resolution and particle identification are needed to ensure success. Much commission of these systems has already been done with cosmic ray events, beam-gas and beam on collimator events [34]. Using dedicated triggers, LHCb will be able to record a huge number of collisions (10^8 events) in only a day of data taking. Using this early data, the K, Λ and D meson signals can be established, and the ratio of track charged measured to within 1%. It may also be possible to measure the $\bar{\Lambda}/\Lambda$ ratio vs η, and distinguish between the predictions of different PYTHIA tunes for strangeness production in fragmentation. These early measurements provide an excellent basis to build the full physics program.

3.3 Jet Measurements

The production of very high energy jets requires a partonic interaction which involves a large fraction of the proton momentum, x. The gluon density at high x has relatively large uncertainties, but recent measurements of inclusive jet cross sections at the Tevatron have added some excellent constraints on this region [35]. The key to these measurements was the unprecedented precision achieved on the jet energy scale at D0 and CDF. Building on these results, D0 and CDF presented a measurements dijet cross section differential in dijet mass [36, 38], comparing the D0 measurement with NLO predictions [37] indicating the high-x gluon distribution can be constrained further, see Figure 8. CDF also interpret the measurement as search for some new resonance decaying to dijets [38], placing limits on various models of new physics. Finally, D0 presented a measurement of the dijet $\chi = e^{y_1+y_2}$ in bins of dijet mass [39]. This measurement is highly sensitive to any new interaction modifying the jet rapidity distribution predicted by QCD. No deviations are observed, and limits are set.

Moving to the LHC, precision jet physics will again rely upon a precise knowledge of the jet energy scale. The methods planned at ATLAS and CMS follow the Tevatron closely: calibrating jets against a recoiling photon or Z boson [29]. To study high x processes, jets much be measured out to very high p_T. In this case, a high p_T jet may be calibrated against several lower p_T recoiling jets. This method will encounter significant systematics, and so it will be challenging for the LHC to compete with Tevatron measurements of high-x gluons. However, even with only a preliminary jet energy scale (10% systematic uncertainty), several interesting measurements are possible. Studies of thrust and $\Delta\phi$(jet, jet) in multi-jet production [40] will allow tuning of the production of multiple jets in ALPGEN [41] and other simulations. The jet p_T, dijet mass and dijet θ^* distributions are all sensitive to new interactions; taking the ratio of central to forward jets cancels several systematics and increases sensitivity [29, 42]. Due to the huge increase in cross sections for new interactions, it is expected the as little as 10 pb^{-1} at 14 TeV will be sufficient to surpass the Tevatron limits. Further, studies of forward jets ($3 < |\eta| < 5$) at CMS [43] are expected to provide an interesting window on the low-x gluon, and non-DGLAP QCD evolution modifying the azimuthal correlation [44].

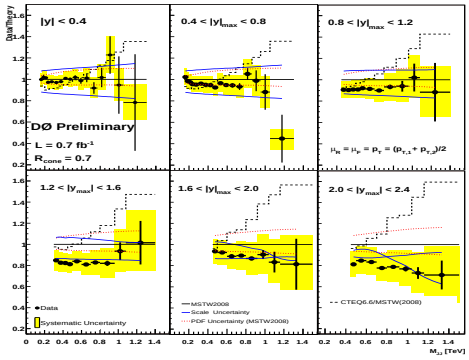

Figure 8: Dijet mass measurement from D0.

3.4 Isolated Photon + Jets Measurements

New Tevatron measurements using photons to probe the proton structure were also presented. In all cases, isolation requirements are used to select prompt photons. CDF have measured the inclusive photon cross section using 2.1 fb^{-1} of data, extending the measured photon p_T range over previous results [45]. Theory [46] agrees with the data except at low p_T, confirming previous observations [47]. D0 look also at photon + jet production, in configurations where the photon and jet have same and opposite sign rapidities [48]. Taking ratios between these various configurations cancels some systematic uncertainties, and highlights the regions where theory is not describing the data. Further, D0 adding heavy flavor tagging to the jet in these photon+jet events, and find theory provides a good description for b jets, but a significant disagreement for c jets [49]. This could be due to a mis-modelling of gluon splitting into $c\bar{c}$, or the charm PDF. Repeating these measurements in the different x region accessible at the LHC will possibly shed some light on this problem.

3.5 W and Z + Jets Measurements

Finally, there were several new measurements of the production of W and Z bosons in association with jets. These events are an excellent testing ground for theoretical predications, and for the main background to processes such as Higgs boson production and some supersymmetric models. In general, NLO pQCD predictions [50] agree well with the measurements from CDF [54] and D0 [51, 52, 53] of the leading, second and third jet p_T, as well as the leading jet rapidity and angles between Z and leading jet, as shown in Figure 9.

D0 also perform extensive comparisons to current event generators [15, 41, 55, 56], which have mixed success in reproducing the data. As leading order simulations, these all have significant uncertainties and some scope for parameter tuning to improve agreement with data. CDF have also measured the first differential $Z + b$ jet cross sections, and see a reasonable description by NLO pQCD; a related measurement of $W + b$ awaits further comparisons to theoretical predictions.

There is an extensive program of W/Z+jets measurements planned at ATLAS and CMS [57], where production cross sections are an order of magnitude larger than at the Tevatron. Measurements W/Z+jets signals can be used to calibrate lepton identification, and improve simulation tuning at LHC energies, where high multiplicity final states will be plentiful. Further, identifying heavy flavor produced in association with a W/Z is an important signal which currently has significant theoretical uncertainties but forms a main background to many Higgs and new physics searches. Studies of W and Z production at LHCb has a different motivation [58]. The differential W/Z cross section at very forward η is sensitive to a region of the PDFs which currently have significant uncertainties. Measuring these cross sections, while challenging, should significantly reduce the PDF uncertainties.

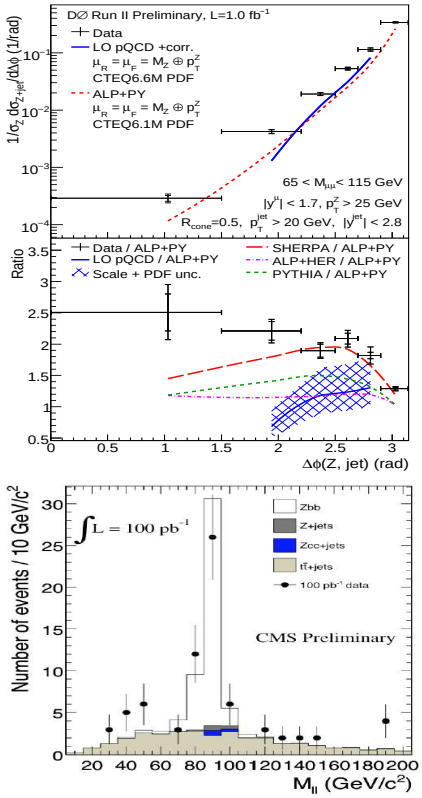

Figure 9: Z+jet measurements from D0 (top), and a $z + b\bar{b}$ study from CMS.

3.6 Summary

There are a wide range of exciting QCD measurements to be made at the energy frontier. The Tevatron experiments have well calibrated detectors, in particular unprecedented levels of precision on the jet energy scale. The QCD program there continues to place tight constraints on PDFs, as well as being an excellent testing ground for theoretical predictions. The high center of mass energy at the LHC will open up a previously unexplored kinematic region, which great possibilities for new discoveries. A huge commissioning effort has been carried out, and collisions are eagerly anticipated.

4 Theory

In the session 18 theory contributions were presented, devoted to several main topics. Two most active topics were gluon resummations and a description of QCD scattering amplitudes

and the final states, within the k_T-factorisation approach, that incorporates a more accurate treatment of parton kinematics. Besides that, important results on fixed order calculations were presented. A few talks in total were devoted to Monte-Carlo implementations of the collinear QCD evolution, the fragmentation functions, and the jet variables. The issues of the underlying event and multiple scattering were not discussed in the session from the theoretical perspective.

4.1 Fixed order calculations

The top quark physics is one of the highlights of the LHC program. An important channel for understanding the kinematical distributions of the top quark is a production of the $t\bar{t}$-pair in association with an additional jet. In particular, this production channel is important source of background in the Higgs boson production through the vector boson fusion. It may also probe the anomalous top quark–gluon coupling. Recently results for this process at the LHC were obtained at the NLO accuracy [59]. The most striking feature of the results is the dependence of the NLO K-factor on the p_T of the top quark. The K-factor decreases with the increasing p_T — from $K \simeq 1.3$ at $p_T = 0$ GeV down to $K \simeq 1$ at $p_T = 300$ GeV, and $K \simeq 0.5$ at $p_T = 600$ GeV. In the current treatment, the natural renormalisation and factorisation scale, μ_0, was assumed to be p_T-independent, $\mu_0 = m_t$, and the theoretical uncertainty was obtained by variations of the scale around μ_0. In this prescription, the theoretical uncertainty of the NLO calculation is significantly reduced w.r.t. the uncertainty of the LO calculation for $p_T < 500$ GeV, but for $p_T > 500$ GeV, those uncertainties become similarly large. This may indicate, that a p_T-dependent choice of the scale would be more adequate.

The Drell–Yan process is one of the best theoretically understood processes in hadron colliders. The fully exclusive cross section for this process is known at the NNLO accuracy with impressive theoretical precision, — the relative theoretical uncertainty reaches the level of a couple per cent. The process may be, therefore, used e.g. as a luminosity monitor at the LHC. In the session, a new NNLO calculation was presented that included a $\gamma - Z^0$ interference, finite width effects of the Z^0-boson leptonic decay of the vector boson and corresponding spin correlations [60]. The calculation provides a valuable cross check of the earlier NNLO calculation. The results are implemented into a publicly available computer code and may be used in practical applications.

4.2 Soft gluon resummations

Radiative corrections to hard scattering of coloured partons due to soft gluons are known to be important, due to large logarithmic enhancement factors. Specifically, at all orders of the perturbative expansion, powers of logarithms emerge of the ratio of two scales: the scale of the hard process μ_H, characteristic for the virtual corrections, and the softer scale, μ_S, that governs the real gluon emissions. When the ratio of the two scales is large, the logarithmically enhanced perturbative corrections should be resummed. The leading soft gluon corrections emerge in the eikonal approximation, in which only the contribution from the leading power of the soft gluon energy is taken into account. The next-eikonal (NE) approximation introduces effects that are suppressed by one power of the soft gluon energy. In the eikonal approximation, the soft gluon effects may be factorized out from the hard scattering amplitude and from non-perturbative effects. Furthermore, the soft gluon corrections then exponentiate and may be resummed using the renormalisation group technique.

The soft gluon resummation may be used to compute improved cross sections for various scattering processes, involving inclusive cross sections for production of colourless particles (e.g. the Drell–Yan process or the Higgs boson production), the p_T dependent differential cross sections or the inclusive cross sections for production of coloured particles, e.g. $t\bar{t}$ pair or dijets.

At the workshop, recent results were presented [61] for the soft gluon resummation beyond the eikonal approximation. The soft gluon logarithms were shown to exponentiate in the next-to-eikonal approximation. The formal proof is based on the path integral formulation of the soft radiation theory.

Another important application of the soft gluon resummations is an improvement of the transverse momentum (q_T) distributions of the heavy particle, with the mass M, produced in hadronic collisions. At the LL level, one resums at the n-th order of the perturbative expansion, the most leading terms $\sim \alpha_s^n \log^{2n-1}(M^2/q_T^2)$, that originate from the soft-collinear logarithms. At the NLL level, one resums terms $\sim \alpha_s^n \log^{2n-2}(M^2/q_T^2)$, coming, in particular, from soft non-collinear logarithms, and NNLL approximation resums terms with a yet lower power of the logarithm. In order to fully exploit the phenomenological consequences of the soft gluon resummation, the resummed cross sections are matched with fixed order calculations. So far, the most advanced calculations were performed for the Higgs boson, where the NNLL resumation was used to improve the NNLO cross section. Recently, an evaluation was performed of the Drell–Yan process at the LO + NLL accuracy [62], and the results at the NLO + NNLL accuracy are expected soon. The soft gluon resummation technique was also used to improve predictions for a recently proposed observable, a_T [63]. a_T is defined as the component of the heavy particle $\vec{q}_T$ perpendicular to the event thrust axis. The choice of the observable a_T, instead of, q_T, may be advantageous from the experimental point of view.

Two interesting applications of the soft gluon resummation were discussed for jet physics. It was proposed, to use the technique to improve the azimuthal decorrelation of the dijets [64]. In particular, the resummation for this observable is particularly useful close to the back-to-back dijet configuration, where the fixed order results diverge, and the resummed cross section is stable. Of particular interest is an ongoing phenomenological study [65] of the non-global superleading logarithms, found before, in the events with two-jet hadroproduction, with a central rapidity region devoid from gluon emissions (the rapidity gap). The super-leading logarithms were found to play a significant rôle if the rapidity gap and the jet transverse momenta are large enough.

4.3 Monte Carlo in the collinear factorisation approach

The standard QCD description of inclusive cross sections in the DIS and in hadronic collisions, is based on the Operator Product Expansion and the collinear factorisation for the leading twist amplitudes. In this framework the partons are assumed to have vanishing transverse momenta. This is, clearly, a significant distortion of the true kinematical situation. A better description of the kinematics may be, however, obtained by inclusion of hard matrix elements with additional emissions or by using higher order calculation. Most of the existing Monte Carlo event generators are based on the collinear formulation. The full final state is then built by representing quark and gluon emissions in the parton evolution by a parton shower.

One of the more important problems in Monte Carlo simulations of the hadronic final

states is a consistent matching of the parton emissions attributed to the hard matrix element with those that occur in the parton shower. In this context, the case of coloured particle production in e^+e^- collisions was considered [66]. The consistent matching was implemented based on the Catani-Krauss-Kuhn-Webber / Lönnblad (CKKW/L) prescription. NLO matrix elements with various particle multiplicities were incorporated. The basic idea of the matching is the transverse momentum separation of the emissions that belong to the parton shower and to the matrix element. An important ingredient of the matching procedure is a suitable application of the multiplicity dependent Sudakov form-factors.

Typically, hadronic cross sections are evaluated in the parton x-space. An alternative approach was proposed, to use the Mellin pseudo-moment representation to perform fast NLO calculation of jet and charm cross sections [67]. This method has been implemented in a numerical package, that can be used in fits of the parton densities.

4.4 k_T-factorisation and exact kinematics

An alternative approach to simulate the final states with the 'collinear Monte Carlo' is provided by the k_T-factorisation framework. In the latter approach transverse momenta of the partons are taken into account along the evolution chain and in all emissions. Therefore, one expects that the treatment of the kinematical details of the final states may be improved with respect to the collinear factorisation framework. On the other hand, the theoretical foundations of k_T-factorisation are not as strong as the ones for the collinear factorisation, as it is not based on a hard factorization theorem. For the bulk of collider events, for which the high energy limit of QCD may be applied, k_T-factorisation is supported by the high-energy (or Regge) factorisation.

CASCADE is a multi-purpose Monte-Carlo code, that uses the concept of k_T-factorisation to simulate cross sections and multi-parton final states in the DIS and in hadronic collisions [68]. It is based on the Catani-Ciafaloni-Fiorani-Marchesini (CCFM) scheme, that resums both Dokshitzer-Gribov-Lipatov-Altarelli-Parisi (DGLAP) logarithms ($\log Q^2$), and the Balitsky-Fadin-Kuraev-Lipatov (BFKL) logarithms ($\log x$) in the evolution of unintegrated parton densities. The feature of angular ordering of gluon emissions incorporated in the CCFM parton shower is motivated by the QCD coherence. The matrix elements are evaluated for off-shell incoming gluons, that carry non-zero transverse momentum. CASCADE was shown to provide a good description of various sets of collider data from HERA and the Tevatron. In particular, angular distributions in three-jet samples are better described by CASCADE than by the collinear factorisation scheme at the NLO [68].

For a long time, only gluonic partons were included in CASCADE. This was sufficient for many applications, as gluon driven processes dominate in the high energy regime. Recently, efforts are made to incorporate also quarks. The sea quarks may be effectively introduced by using suitable matrix elements. For instance, the vector boson, V, production (where $V = \gamma^*$, Z^0 or $W^{\pm}$) may be treated within the k_T-factorisation approach by evaluating suitable off-shell matrix elements with quarks, i.e. $g^*g^* \to q\bar{q}V$. The valence quark CCFM evolution was also implemented. Then, the quark-gluon contribution to the forward jet production was introduced into CASCADE [69]. In addition, possible effects of unitarity corrections in the CCFM evolution of the unintegrated gluon density were investigated using an approximate 'absorptive boundary' prescription [68]. In a separate study, the formalism based on the k_T-factorisation was applied to compute the differential cross sections of $W^{\pm}$ and Z^0 production at the Tevatron [70]. In addition, an extensive analysis of the the prompt

photon and diphoton production at HERA and at the Tevatron was performed [71]. In all the cases, a satisfactory overall description of the data was obtained.

A rather interesting application of the k_T-factorisation was presented to the case of the Higgs boson production at the LHC, together with multiple jets [72]. The description of multiple jet emission in the Higgs boson production was based on the leading logarithmic BFKL approximation. The approximation was further improved, by inclusion of the longitudinal degrees of freedom in the gluon propagators and the emission vertexes. After this improvement was applied, the obtained results for lower number of jets were found to agree well with ones obtained with the exact matrix elements. A code with a Monte-Carlo implementation of the technique is readily available.

The high energy gluon-gluon scattering and fragmentation was studied in detail using the light-front quantisation formalism, in which no kinematical approximation was made [73]. Several interesting results were derived in the large N_c limit: the exact form of the tree level gluon light-cone wave function and the multi-gluon final state were obtained for the gluon configurations with the maximal helicity violation (MHV). In addition the analysis lead to a phenomenological prescription for the (necessary) resummation of multiple collinear logarithms, found e.g. in the NLL BFKL kernel.

4.5 Fragmentation and jets

Inclusive distribution of a single hadron emerging from hard scattering are described by combining a suitable hard matrix element with a fragmentation function. The fragmentation function is universal and evolves with the process scale according to a perturbative evolution equation, and the non-perturbative contribution is absorbed into the initial condition of the evolution. This approach, at the NLO accuracy, was used to describe HERA data on single π^0 and $D^{\pm}$ production in the neutral current DIS [74]. In the analysis the Albino-Kniehl-Kramer (AKK) and Kniehl-Kramer-Schienbein-Spiesberger (KKSS) fragmentation functions were used. The Z^0 contribution was also calculated and found to be small (up to a few per-cent level at the highest Q^2). A good description of the data was obtained.

In scattering processes on nuclei, the jet-partons are typically produced inside the nucleus. It is, therefore, expected, that the fragmentation process of a parton to a hadron is affected by the nuclear medium. Indeed, the data show effects of the medium that increase with the increasing atomic mass number A. A wide set of data for pion, kaon and proton production off various nuclei was analyzed, and the in-medium fragmentation functions were fitted [75]. It was assumed in the analysis that the medium effects occur mostly at low scales, hence they do not affect the evolution. Therefore, the standard NLO evolution of the fragmentation functions was used, and the medium effects were represented by the fitted initial condition of the evolution. A good fit to the pion data was obtained, but the description of kaon and proton data was less precise.

The issue of jet variables was discussed in only one talk. A correction to jet p_T was considered coming from the non-perturbative effects related to the hadronization process [76]. The jet data support a phenomenological description of the effect using a concept of an effective drag force. It emerges due to universal non-perturbative emissions. This model was applied to compute the modification $\langle \delta p_T \rangle$ of jet p_T due to hadronization, for various jet algorithms and as a function of jet cone size, R. A simple result was found, $\langle \delta p_T \rangle \simeq -0.5\mathcal{M}/R$ GeV, with $\mathcal{M} = 1$ – 1.5, depending on the jet algorithm.

Acknowledgments

L. M. is supported by the DFG grant No. SFB 676 and by the Polish Ministry of Education grant No. N202 249235.

References

[1] Slides: `http://indico.cern.ch/contributionDisplay.py?contribId=329&sessionId=22&materialId=slides&confId=53294`

[2] Claire Gwenlan, these proceedings.

[3] Arnd Specka, these proceedings.

[4] Elias Ron, these proceedings.

[5] Stephen Magill, these proceedings.

[6] Krzysztof Nowak, these proceedings.

[7] Matthew Forrest, these proceedings.

[8] A. V. Lipatov and N. P. Zotov, Phys. Rev. D **72**, 054002 (2005).

[9] M. Fontannaz, J. P. Guillet and G. Heinrich, Eur. Phys. J. C **21**, 303 (2001).

[10] A. Gehrmann-De Ridder, T. Gehrmann and E. Poulsen, Phys. Rev. Lett. **96**, 132002 (2006).

[11] A. D. Martin *et al.* Eur. Phys. J. C **39**, 155 (2005)

[12] Dan Traynor, these proceedings.

[13] John Morris, these proceedings.

[14] Lluis Martii, these proceedings.

[15] T. Sjöstrand, S. Mrenna, and P. Skands, JHEP **05**, 026 (2006).

[16] H. Jung, Comput. Phys. Commun. **143**, 100 (2002) and Hannes Jung, these proceedings.

[17] Deniz Sunar, these proceedings.

[18] H1 Collaboration, F. D. Aaron *et al.*, Eur. Phys. J. C **61** 185 (2009), and Grazyna Nowak, these proceedings.

[19] L. Lonnblad, Comput. Phys. Commun. **71**, 15

[20] H1 Collaboration, F. D. Aaron *et al.*, Phys. Lett. B **673**, 119 (2009), and Anna Kropivnitskaya, these proceedings.

[21] ZEUS Collaboration, S. Chekanov *et al.*, Phys. Rev. Lett. **101** 112003 (2008), and David Saxon, these proceedings

[22] Yves van Haarlem, these proceedings.

[23] Ken Hicks, these proceedings.

[24] CLAS Collaboration K. S. Egiyan *et al.*, Phys. Rev. Lett. **96**, 082501 (2006), and Yordanka Ilieva, these proceedings.

[25] Steffen Strauch, these proceedings.

[26] Lars Sonnenschein, these proceedings.

[27] Christina Mesropian, these proceedings.

[28] CDF Collaboration, T. Affolder *et al.*, Phys. Rev. D **65**, 092002 (2002).

[29] Craig Buttar, these proceedings.

[30] Nick van Remortel, these proceedings.

[31] Luca Mucibello, these proceedings.

[32] M. G. Albrow *et al.*, arXiv:0610012 [hep-ph] (2006).

[33] J. M. Butterworth, J. R. Forshaw, and M. H. Seymour, Z. Phys. C **72**, 637 (1996).

[34] Markward Britch, these proceedings.

[35] A. D. Martin, W. J. Stirling, R. S. Thorne, and G. Watt, arXiv:0901.0002v2 [hep-ph] (2009).

[36] Mandy Rominsky, these proceedings.

[37] T. Kluge, K. Rabbertz, and M. Wobisch, arXiv:hep-ph/0609285.

[38] Phys. Rev. D. **79**, 12002 (2009), and Mario Martinez, these proceedings.

[39] Nirmalya Parua, these proceedings.

[40] Matthias Artur Weber, these proceedings.

[41] M. L. Mangano *et al.*, JHEP **0307**, 001 (2003).

[42] Andreas Oehler, these proceedings.

[43] Salim Cerci, these proceedings.

[44] A.H.Mueller, H.Navelet, Nucl.Phys. B **282**, 727 (1987).

[45] Carolina Deluca, these proceedings.

[46] S. Catani *et al.*, JHEP **0205**, 028 (2002).

[47] D0 Collaboration, V. M. Abazov *et al.*, Phys. Lett. B 658, 285 (2008).

[48] D0 Collaboration, V. M. Abazov *et al.*, Phys. Lett. B **666**, 2435 (2008), and Lars Sonnenschein, these proceedings.

[49] D0 Collaboration, V. M. Abazov *et al.*, Phys. Rev. Lett. **102**, 192002 (2009), and Lars Sonnenschein, these proceedings.

[50] J. Campbell and R. K. Ellis, Phys. Rev. D **65**, 113007 (2002).

[51] D0 Collaboration, V. M. Abazov *et al.*, Phys. Lett. B **699**, 278 (2008).

[52] D0 Collaboration, V. M. Abazov *et al.*, Phys. Lett. B **658**, 112 (2008).

[53] Michael Kirby, these proceedings.

[54] CDF Collaboration, T. Affolder *et al.*, Phys. Rev. Lett. **100**, 102001 (2008), and Tara Shears, these proceedings.

[55] G. Corcella *et al.*, JHEP **0101**, 010 (2001).

[56] T. Gleisberg *et al.*, JHEP **0902**, 007, 2009.

[57] Jason Nielson, these proceedings.

[58] Sarah Traynor, these proceedings.

[59] P. Uwer, these proceedings.

[60] M. Grazzini, these proceedings, the talk on the Drell-Yan process.

[61] C. White, these proceedings, the talk on the soft gluon resummation.

[62] M. Grazzini, these proceedings, the talk on the p_T-resummation.

[63] R. Delgado, these proceedings.

[64] A. Banfi, these proceedings.

[65] S. Marzani, these proceedings.

[66] L. Lönnblad, these proceedings.

[67] H. Kawamura, these proceedings.

[68] H. Jung, these proceedings.

[69] M. Deak, these proceedings.

[70] N. Zotov, these proceedings.

[71] V. Saleev, these proceedings.

[72] C. White, these proceedings, the talk on the Higgs boson plus jet production.

[73] A. Staśto, these proceedings.

[74] C. Sandoval, these proceedings.

[75] R. Sassot, these proceedings.

[76] Y. Delenda, these proceedings.